

# Action Transformer: A Self-Attention Model for Short-Time Human Action Recognition

Vittorio Mazzia<sup>1,2,3</sup>, Simone Angarano<sup>1,2</sup>, Francesco Salvetti<sup>1,2,3</sup>, Federico Angelini<sup>4</sup> and Marcello Chiaberge<sup>1,2</sup>

<sup>1</sup> Department of Electronics and Telecommunications, Politecnico di Torino, 10124 Turin, Italy

<sup>2</sup> PIC4SeR, Politecnico di Torino Interdepartmental Centre for Service Robotics, Turin, Italy

<sup>3</sup> SmartData@PoliTo, Big Data and Data Science Laboratory, Turin, Italy

<sup>4</sup> School of Computing, Newcastle University, 1 Science Square, Newcastle, NE45TG, UK

**Abstract**—Deep neural networks based purely on attention have been successful across several domains, relying on minimal architectural priors from the designer. In Human Action Recognition (HAR), attention mechanisms have been primarily adopted on top of standard convolutional or recurrent layers, improving the overall generalization capability. In this work, we introduce Action Transformer (AcT), a simple, fully self-attentional architecture that consistently outperforms more elaborated networks that mix convolutional, recurrent, and attentive layers. In order to limit computational and energy requests, building on previous human action recognition research, the proposed approach exploits 2D pose representations over small temporal windows, providing a low latency solution for accurate and effective real-time performance. Moreover, we open-source MPOSE2021, a new large-scale dataset, as an attempt to build a formal training and evaluation benchmark for real-time short-time human action recognition. Extensive experimentation on MPOSE2021 with our proposed methodology and several previous architectural solutions proves the effectiveness of the AcT model and poses the base for future work on HAR.

## I. INTRODUCTION

The Transformer architecture, proposed by [37], has been one of the most important deep learning introductions for natural language processing (NLP) of the last years. Moreover, multi-head self-attention has proven to be effective for a wide range of tasks besides NLP, from image classification [15], generative adversarial networks [24] to speech recognition [8]. Moreover, optimized versions of the Transformer have been developed for real-time, and embedded applications [8], proving that this architecture is also suitable for Edge AI purposes. Recently, many attention models have also been applied to Human Action Recognition (HAR) to improve the accuracy of models primarily based on convolutions and recurrent blocks. However, fully self-attentional solutions have not been investigated for this task yet.

In this paper, inspired by the simple and priors-free architecture of the Vision Transformer [15], we apply a pure Transformer encoder derived architecture to the action recognition task, obtaining an accurate and low-latency model for real-time applications (Fig. 1). We use the new single-person short-time action recognition dataset MPOSE2021

This work has been developed with the contribution of the Politecnico di Torino Interdepartmental Centre for Service Robotics PIC4SeR (<https://pic4ser.polito.it>) and SmartData@Polito (<https://smartdata.polito.it>).

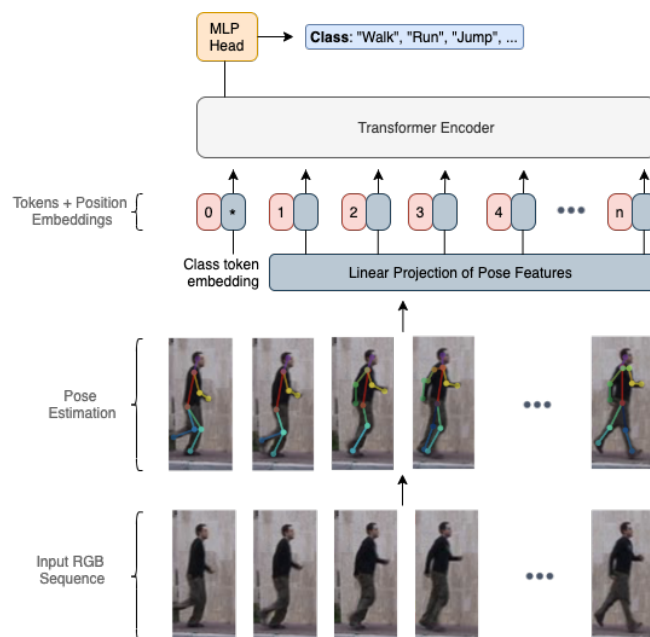


Fig. 1. Overview of the Action Transformer architecture. Pose estimations are linearly projected to the dimension of the model, and together with the class token, they form the input tokens for the transformer encoder. As with Vision Transformer models [15], [36], a learned position embedding is added to each input token, and exclusively the class token is passed through a multi-layer perceptron head to make the final class prediction.

and exploit 2D human poses representations provided by two existing methodologies: OpenPose [9] and PoseNet [28]. Moreover, we compare our trained models with other state-of-the-art solutions and baselines to highlight the advantages of the proposed approach.

The main contributions of this work can be summarized as follows:

- We study the application of the Transformer encoder to 2D pose-based HAR and propose the novel Action Transformer (AcT) model, proving that fully self-attentional architectures outperform other existing convolutional and recurrent models for the HAR task.
- We introduce MPOSE2021, a dataset for real-time short-time HAR, suitable for both pose-based and RGB methodologies. It includes more than 15000 sequences from different actors and scenarios with a limited num-

ber of frames per scene. In contrast to other publicly available datasets, the peculiarity of having a constrained number of time steps stimulates the development of actual real-time methodologies that perform HAR with low latency and high throughput.

- We conduct extensive experimentation on model performance and latency to verify the suitability of AcT for real-time applications and pave the way for future work on this theme.

The rest of the paper is organized as follows. Section II briefly reports the principal research works on HAR and self-attention deep learning methodologies. Section III presents the dataset MPOSE2021, highlighting its most important features and elements of novelty with respect to other existing datasets. Then, Section IV describes the architecture of the proposed AcT model, shortly recalling the main features of the Transformer encoder. Section V summarizes all the experimentation conducted to verify the effectiveness of the proposed approach, gives a visual insight into the functioning of the model, studies its behavior under temporal information reduction, and measures its latency for real-time applications. Section VI draws some conclusions for this work and indicates future directions.

## II. RELATED WORKS

Human Action Recognition algorithms aim at detecting and classifying human behaviors based on a different source of information. Works in this field can be mainly subdivided into two broad categories: video-based and skeleton-based methodologies [34]. In this second approach, the input consists of a sequence of points representing body joints, usually associated with a corresponding RGB frame. Skeletons can be represented in the 3D space, such as those generated with Kinetic sensors [31], [25], or in the 2D space of the image view [22], [40]. In this work, we focus on 2D pose information since it can be directly obtained from an image

by pose detection algorithms such as OpenPose [9] and PoseNet [28]. This characteristic makes 2D HAR methodologies applicable in a great range of applications using a simple RGB camera. At the same time, 3D information would require particular sensors, such as the Kinect, that present strong limitations, such as the availability, the cost, the effective working range (up to 5-6 meters) [23] and the performance degradation in outdoor environments. Angelini et al. first collect the MPOSE dataset [2], [3], obtaining 2D poses processing several popular HAR video datasets with OpenPose. Moreover, the authors proposed ActionXPose, a methodology mainly based on MLSTM-FCN [21] to classify poses with a combination of 1D convolutions, LSTM [19] and Squeeze-and-excitation attention [20]. The same authors successively applied their approach to anomaly detection [5], [4] and expanded the MPOSE collection with the novel ISLD and ISLD-Additional-Sequences datasets. Yan et al. [40] first applied OpenPose to extract 2D poses from the Kinetics-400 RGB dataset [22] and used graph convolutions to capture both spatial and temporal information. Shi et al. [32], [33] applied graph convolutions to pose information using two streams that extract information from both joints and bones to represent the skeleton. Liu et al. [26] proposed an ensemble of two independent bone-based and joint-based models using a unified spatial-temporal graph convolutional operator. Cho et al. [13] first applied self-attention [37] to the skeleton-based HAR problem. More recently, Plizzari et al. [29], inspired by Bello et al. [7], employed self-attention to overcome the locality of the convolutions, again adopting a two-stream ensemble method, where self-attention is applied on the temporal and spatial information, respectively.

Unlike these previous methodologies, in this paper, inspired by works in the field of image classification [15] and speak recognition [8], we first present an architecture for HAR entirely based on the Transformer encoder [37], without any convolutional or recurrent layer. Moreover, we focus on the model latency to verify its suitability for real-time applications. For this reason, we introduce a new 2D pose-based dataset specifically designed for short-time HAR. Unlike the traditional datasets used by previous works, such as the 3D NTU RGB+D [31], [25], or the Kinetics-Skeleton [22], [40], the MPOSE2021 dataset collects poses with a temporal duration of 30 frames, making it a new possible benchmark to test real-time performances of HAR methodologies.

## III. THE MPOSE2021 DATASET

In this section, MPOSE2021 is presented as an RGB-based dataset designed for short-time, pose-based HAR. Inspired by [3], [5], [4], video data were previously collected from popular HAR datasets (precursors), i.e. Weizmann [17], i3DPost [16], IXMAS [38], KTH [30], UTKinetic-Action3D (RGB only) [39] and UTD-MHAD (RGB only) [11], ISLD and ISLD-Additional-Sequences [3].

Due to the heterogeneity of action labels across different datasets, class labels are remapped to a list of 20 common classes. Actions that cannot be remapped accordingly are

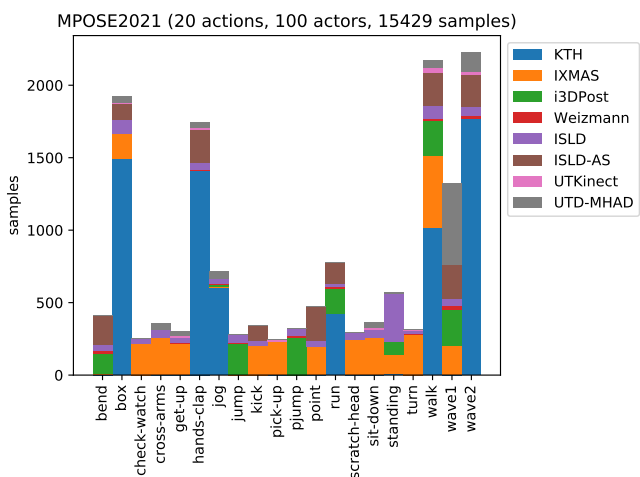


Fig. 2. MPOSE2021 number of samples by action for each sub-dataset. The overall dataset accounts more than 15000 samples divided in 20 separate classes and performed by 100 distinct actors.

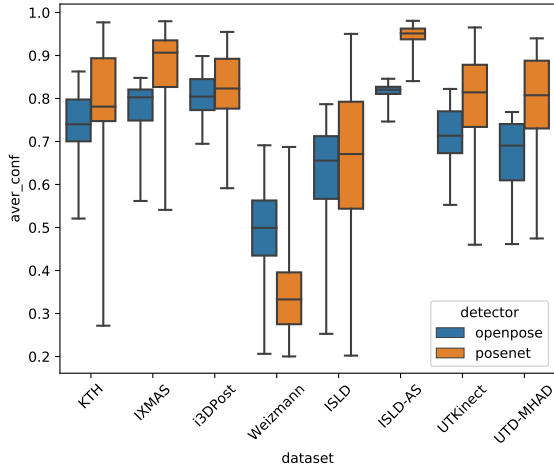


Fig. 3. Comparison between OpenPose and PoseNet average confidence (aver\_conf) by MPOSE2021 sub-dataset. The detectors achieve different average confidence based on the considered precursor dataset.

discarded. Therefore, precursor videos are divided into non-overlapping samples (clips) of 30 frames each whenever possible and retaining tail samples with more than 20 frames. A visual representation of the number of samples by action for each sub-dataset of MPOSE2021 is shown in Fig. 4. The peculiarity of a reduced number of time steps contrasts with other publicly available datasets and stimulates the development of methodologies that require low latency to perform a prediction. That would largely benefit many real-world applications requiring real-time perception of the actions performed by humans nearby.

Subsequently, clips not containing a single action are discarded. Moreover, ambiguous clips are relabelled whenever possible or discarded otherwise. This process leads to 15429 samples, where each sample represents a single actor performing a single action. The total number of distinct actors in MPOSE2021 is 100 (Fig. 2).

OpenPose [9] and PoseNet [28] are used to extract landmarks from MPOSE2021 samples. For each sample, the average confidence is computed as the mean of the landmarks' confidence across landmarks and frames. It turns out that the two detectors achieve different average confidence based on the considered precursor dataset. The comparison statistics are described by the box plot of Fig. 3).

Due to the significant sample heterogeneity and the high number of actors, three different training/testing splits are defined for MPOSE2021, i.e., Split1, Split2, and Split3, by randomly selecting 21 actors for testing and using the rest of them for training. The three splits division makes the proposed dataset a challenging benchmark to effectively assess and compare the accuracy and robustness of different methodologies. Moreover, the suggested evaluation procedure requires testing a target model on each split using ten different validation folds and averaging the obtained results together. That makes it possible to produce statistics and reduces the possibility of overfitting the split testing set with an accurate choice of hyperparameters.

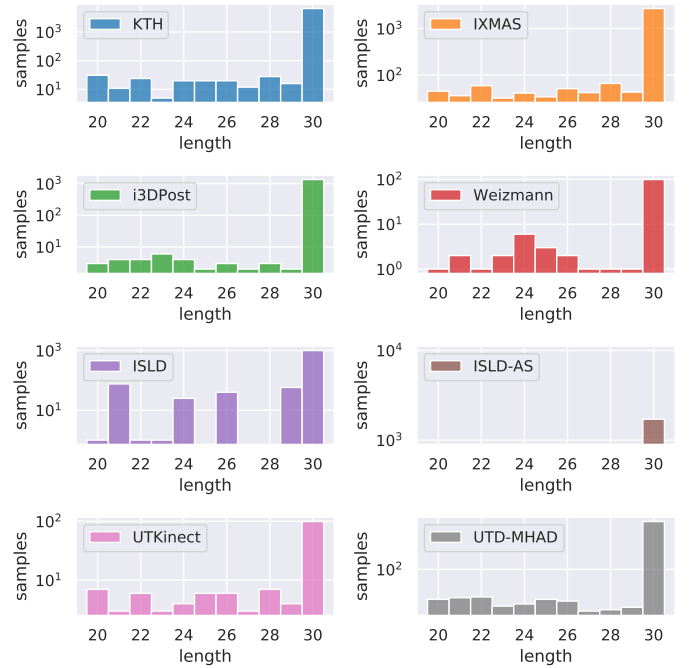


Fig. 4. MPOSE2021 number of frames (length) distributions by sub-dataset. It is possible to notice how the majority of the sub-dataset presents an average of 30 frames per scene.

With MPOSE2021, we aim at providing an end-to-end and easy-to-use benchmark to robustly compare state-of-the-art methodologies for the short-time human action recognition task. We thus release a curated code repository to access the different levels of the dataset: Video data, 2D poses, and RGB + 2D poses. Moreover, we open source a practical Python package to access 2D poses, visualize and preprocess them with standard functions. The Python package can be easily installed with "pip install mpose". All source code and instructions can be found at [https://github.com/FedericoAngelini/MPOSE2021\\_Dataset](https://github.com/FedericoAngelini/MPOSE2021_Dataset).

#### IV. ACTION TRANSFORMER

In this section, we describe in detail the architecture of the AcT network, summarized in Fig. 1, briefly recalling preliminaries associated with the Transformer model [37].

##### A. AcT Architecture

A  $i$ -th video input sequence with  $T$  frames of dimension  $H \times W$  and  $C$  channels,  $\mathbf{X}_{rgb} \in \mathbb{R}^{T \times H \times W \times C}$ , is pre-processed by a multi-person 2D pose estimation network

$$\mathbf{X}_{2Dpose} = F_{2Dpose}(\mathbf{X}_{rgb}) \quad (1)$$

that extracts 2D poses of dimension  $N \times T \times P$ , where  $N$ , is the number of human subject present in the frame and  $P$  is the number of keypoints predicted by the network. The Transformer architecture receives as input a 1D sequence of token embeddings, so each  $N$  sequence of poses matrix,  $\mathbf{X}_{2Dpose} \in \mathbb{R}^{T \times P}$ , is separately processed by the AcT network. Nevertheless, at inference time, all detected poses in the video frame can be batch processed by the AcT model,

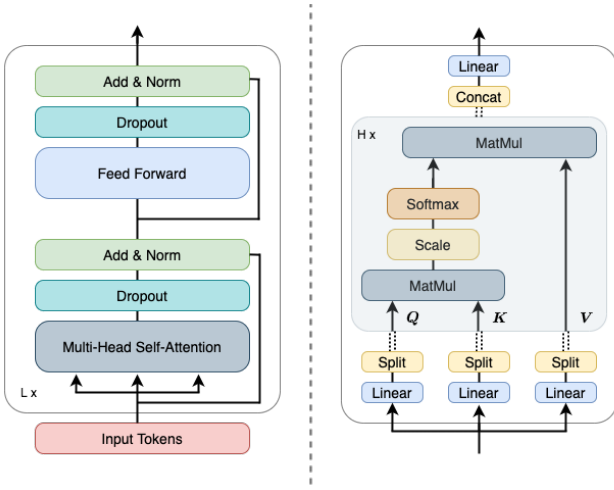


Fig. 5. Transformer encoder layer architecture (left) and schematic overview of a multi-head self-attention block (right). Input tokens go through  $L$  encoder layers and  $H$  self-attention heads.

simultaneously producing a prediction for all  $N$  subjects. Firstly, each  $T$  keypoint predictions are mapped to a higher dimension  $D_{model}$  using a linear projection map  $\mathbf{W}^{l_0} \in \mathbb{R}^{P \times D_{model}}$ . As in BERT [14] and Vision Transformers (ViT) derived researches [15], [36], [8], [10] a trainable vector of dimension  $D_{model}$  that goes through the transformer layers is added to the input  $T$  sequence. This class token [CLS] forces the self-attention to spread information between the input sequence and aggregates their information into a high-dimensional representation that separates the different action classes. Moreover, a positionality information is provided to the sequence with a learnable positional embedding matrix  $\mathbf{X}_{pos} \in \mathbb{R}^{(T+1) \times D_{model}}$  added to all tokens.

The set of linearly projected tokens and [CLS] token are fed to a standard Transformer encoder,  $F_{TEnc}$ , of  $L$  layers with a "post-norm" layer normalization [37], [12], as

$$\mathbf{X}^L = F_{TEnc}(\mathbf{X}^{l_0}) = F_{TEnc}([\mathbf{x}_{cls}^{l_0}; \mathbf{X}_{2Dpose}] + \mathbf{X}_{pos}) \quad (2)$$

where  $\mathbf{X}^L \in \mathbb{R}^{(T+1) \times D_{model}}$  is the overall representation produced by the Transformer encoder at its last layer. Finally, only the [CLS] token,  $\mathbf{x}_{cls}$ , is fed into a linear classification head,  $MLP_{head}$ , that performs the final class prediction

$$\hat{\mathbf{z}} = MLP_{head}(\mathbf{x}_{cls}^L) \quad (3)$$

where  $\hat{\mathbf{z}}$  are the output logits of the AcT model. At training time the supervision signal comes only from the [CLS] token, while all remaining  $T$  tokens are the model's only variable input. It is important to notice how the nature of the network makes it possible to accept a reduced number of frames as input even if trained with a fixed  $T$ . That gives an additional degree of freedom at inference time, making the AcT network more prone to adapt to different applications than other literature models.

The resulting network is a lightweight solution capable of predicting actions for multiple persons in a video stream with high accuracy. The advantage of building on 2D pose

TABLE I  
ACTION TRANSFORMER PARAMETERS OF THE FOUR VERSION SIZES.

Model	H	$D_{model}$	$D_{mlp}$	L	Parameters
AcT- $\mu$	1	64	256	4	227k
AcT-S	2	128	256	5	1,040k
AcT-M	3	192	256	6	2,740k
AcT-L	4	256	512	6	4,902k

estimations enables effective real-time performance with low latency and energy consumption.

### B. Transformer Architecture

The Transformer encoder [37] is made of  $L$  layers with alternating multi-headed self-attention and feed-forward blocks. Dropout [35], LayerNorm [6] and residual connections are applied after every block. The overall sequence of blocks of a Transformer encoder is summarized on the left of Fig. 5.

Each feed-forward block is a multi-layer perceptron with two layers, and GeLu [18] as non-linearity. The first layer expands the dimension from  $D_{model}$  to  $D_{mlp} = 4 \cdot D_{model}$  and applies the non-linearity. On the other hand, the second layer reduces the dimension back from  $D_{mlp}$  to  $D_{model}$ .

Instead, the multi-head  $QKV$  self-attention mechanism (MSA) is based on a trainable associative memory with key, value vector pairs. For the  $l$ -th layer of the Transformer encoder and the  $h$ -th head, queries ( $Q$ ), keys ( $K$ ) and values ( $V$ ) are computed as  $Q^l = X^l W_Q^l$ ,  $K^l = X^l W_K^l$  and  $V^l = X^l W_V^l$  respectively, where  $W_Q^l$ ,  $W_K^l$  and  $W_V^l$  belong to  $\mathbb{R}^{D_{model} \times D_h}$  with  $D_h$  the dimensionality of the attention head. So, for each self-attention head (SA) and each element in an input sequence  $X^l \in \mathbb{R}^{T \times D_{model}}$ , we compute a weighted sum over all values  $V^l$  in the sequence. The attention weights  $A_{ij}$  are derived from the pairwise similarity between two elements of the sequence and two elements of the sequence and their respective query  $Q_i^l$  and key  $K_j^l$  representation. Therefore, it is possible to compute the attention weights,  $A \in \mathbb{R}^{T \times T}$ , for the  $l$ -th layer as

$$A = \text{Softmax} \left( \frac{QK^T}{\sqrt{D_H}} \right) \quad (4)$$

and the final weighted sum SA as

$$SA(X) = AV \quad (5)$$

Finally, we perform a SA operation for each head of the  $l$ -th layer. We concatenate the results and linearly project the output tensor to the original dimension model as

$$MSA(X) = [SA_1(X); SA_2(X); \dots; SA_H(X)] W_{MSA} \quad (6)$$

where  $W_{MSA} \in \mathbb{R}^{H \cdot D_h \times D_{model}}$ . All operations are schematized on the right side of Fig. 5. The input tensor  $X^l$  is firstly projected to  $T \times H \cdot D_h$  and then a SA operation is performed to all  $H$  split of the resulting projected tensor. Finally, all head outputs are concatenated and linearly projected back to  $D_{model}$ . So, the attention mechanism takes place in the time-domain, allowing different time windows to attend each other and form a global representation in the class embedding.

TABLE II  
HYPERPARAMETERS USED IN ACT EXPERIMENTS.

Training		Regularization	
Training epochs	350	Weight decay	1e-4
Batch size	512	Label smoothing	0.1
Optimizer	AdamW	Dropout	0.3
Warmup epochs	40%	Random flip	50%
Step epochs	80%	Random noise $\sigma$	0.03

In order to reduce the number of hyperparameters and linearly scale the dimension of the AcT model, we fix  $D_{model}/H = 64$ , varying  $H$ ,  $D_{mlp}$  and  $L$  to obtain a different version of the AcT network. In particular, in Table I, we summarized the four AcT versions with their respective number of parameters. The four models, micro, small, medium, and large, primarily differ for their number of heads and layers that substantially increase the number of trainable parameters.

## V. EXPERIMENTS

In this section, we describe the main experiments conducted to study the advantages of using a fully self-attentional model for 2D pose-based HAR. First, the four variants of AcT described in Section IV are compared to existing state-of-the-art methodologies and baselines on MPOSE2021. Then, we further analyze the behavior of the network in order to get a visual insight of the attention mechanism and study the performance under a reduction of the temporal information. Finally, we study model latency for all the designed architectures with two different CPU types, proving that AcT can easily be used for real-time applications.

### A. Experimental Settings

In the following experiments, we employ both the OpenPose and PoseNet versions of the MPOSE2021 dataset. Either set of data have  $T = 30, 52$ , and  $68$  features, respectively. The training set is composed of  $9421$  samples and  $2867$  for testing. The remaining  $3141$  instances are used as validation to find the most promising hyperparameters with a grid search analysis. All results, training, and testing code for the AcT model are open source and publicly available<sup>1</sup>.

Table I are summarized all hyperparameters for the four versions of the AcT architecture, and in Table II all settings related to the training procedure. The AdamW optimization algorithm [27] is employed for all training with the same scheduling proposed in [37], but with a step drop of the learning rate  $\lambda$  to  $1e-4$  at a fixed percentage of the total number of epochs. We employ the TensorFlow 2<sup>2</sup> framework to train the proposed network on a PC with 32-GB RAM, an Intel i7-9700K CPU, and an Nvidia 2080 Super GP-GPU. Following the MPOSE2021 defined benchmark strategy, the total training procedure for the four version sizes takes approximately 32 hours over the three different splits. We

<sup>1</sup><https://github.com/Act>

<sup>2</sup><https://www.tensorflow.org>

exploit publicly available code for what concerns other state-of-the-art models and use the same hyperparameters and optimizer settings described by the authors in almost all the cases. The only exception is made for learning rate, epochs number, and batch size to adapt the methodologies to our dataset and obtain better learning curves.

### B. Action Recognition on MPOSE2021

We run extensive experimentation on MPOSE2021 considering some baselines, common HAR architectures, and our proposed AcT models. We report the mean and standard deviation of 10 models trained using different validation splits to obtain statistically relevant results. The validation splits are kept constant for all the models and correspond to 10% of the train set selected to maintain the same class distribution. The benchmark is executed for both OpenPose and PoseNet data and repeated for all the three train/test splits provided by MPOSE2021. The baselines chosen for the benchmark are a Multilayer Perceptron (MLP), a fully convolutional model (Conv1D), and REMNet, which is a more sophisticated convolutional network with attention and residual blocks proposed in [1] for time series feature extraction. Moreover, four popular models used for multivariate time series classification and, in particular, HAR are reproduced and tested. Among those, MLSTM-FCN [21] combines convolutions, spacial attention, and an LSTM block, and its improved version ActionXPose [2] uses additional preprocessing, leading the model to exploit more correlations in data. MS-G3D [26] makes use of spatial-temporal graph convolutions to make the model aware of spatial relations between skeleton keypoints, while ST-TR [29] joins graph convolutions with Transformer-based self-attention applied both to space and time. As the last two solutions also propose a model ensemble solution, these results are further compared to AcT ensembles made of 2, 5, and 10 single-shot models. We also report the achieved balanced accuracy for each model and use it as the primary evaluation metric to account for the uneven distribution of classes.

The results of the experimentation for OpenPose are summarized in Table III. The fully convolutional baseline strongly outperforms the MLP, while REMNet proves that introducing attention and residual blocks further increases accuracy. As regards MLSTM-FCN and ActionXPose, it is evident that explicitly modeling both spatial and temporal correlations, made possible by the two separate branches, slightly improves the understanding of actions with respect to models like REMNet. MS-G3D, in its joint-only (J) version, brings further accuracy improvement by exploiting graph convolutions and giving the network information on the spatial relationship between keypoints. On the other hand, ST-TR shows performance comparable with all other single-shot models, despite, as MS-G3D, taking advantage of graph information.

The proposed AcT model demonstrates the potential of pure Transformer-based architectures, as all four versions outperform other methodologies while also showing smaller standard deviations. Moreover, even the smallest AcT- $\mu$

TABLE III

BENCHMARK OF DIFFERENT MODELS FOR SHORT-TIME HAR ON MPOSE2021 SPLITS USING OPENPOSE 2D SKELETAL REPRESENTATIONS.

MPOSE2021 Split		OpenPose 1		OpenPose 2		OpenPose 3	
Model	Parameters	Accuracy [%]	Balanced [%]	Accuracy [%]	Balanced [%]	Accuracy [%]	Balanced [%]
MLP	1,334k	82.66 ± 0.33	74.56 ± 0.56	84.41 ± 0.60	74.58 ± 1.00	83.48 ± 0.58	76.60 ± 0.77
Conv1D	4,037k	88.18 ± 0.64	81.97 ± 1.40	88.93 ± 0.43	80.49 ± 0.95	88.67 ± 0.38	83.93 ± 0.58
REMNet [1]	4,211k	89.18 ± 0.51	84.20 ± 0.84	88.77 ± 0.35	80.29 ± 0.88	89.80 ± 0.59	86.18 ± 0.40
ActionXPose [2]	509k	87.60 ± 0.98	82.13 ± 1.50	88.42 ± 0.70	81.28 ± 1.40	89.96 ± 1.00	86.65 ± 1.60
MLSTM-FCN [21]	368k	88.62 ± 0.74	83.55 ± 0.88	90.19 ± 0.68	83.84 ± 1.20	89.80 ± 0.94	87.33 ± 0.67
T-TR [29]	3,036k	87.72 ± 0.87	81.99 ± 1.64	88.14 ± 0.53	80.23 ± 1.19	88.69 ± 0.95	85.03 ± 1.60
MS-G3D (J) [26]	2,868k	89.90 ± 0.50	85.29 ± 0.98	90.16 ± 0.64	83.08 ± 1.10	90.39 ± 0.44	87.48 ± 1.20
AcT- $\mu$	227k	90.86 ± 0.36	86.86 ± 0.50	91.00 ± 0.24	85.01 ± 0.51	89.98 ± 0.47	87.63 ± 0.54
AcT-S	1,040k	91.21 ± 0.48	87.48 ± 0.76	91.23 ± 0.19	85.66 ± 0.58	90.90 ± 0.87	88.61 ± 0.73
AcT-M	2,740k	<b>91.38 ± 0.32</b>	<b>87.70 ± 0.47</b>	91.08 ± 0.48	85.18 ± 0.80	91.01 ± 0.57	88.63 ± 0.51
AcT-L	4,902k	91.11 ± 0.32	87.27 ± 0.46	<b>91.46 ± 0.42</b>	<b>85.92 ± 0.63</b>	<b>91.05 ± 0.80</b>	<b>89.00 ± 0.74</b>
ST-TR [29]	6,072k	89.20 ± 0.71	83.95 ± 1.11	89.29 ± 0.81	81.53 ± 1.39	90.49 ± 0.53	87.06 ± 0.70
MS-G3D (J+B) [26]	5,735k	91.13 ± 0.33	87.25 ± 0.50	91.28 ± 0.29	85.10 ± 0.50	91.42 ± 0.54	89.66 ± 0.55
AcT- $\mu$ (x2)	454k	91.76 ± 0.29	88.27 ± 0.37	91.34 ± 0.40	86.88 ± 0.48	91.70 ± 0.57	88.87 ± 0.37
AcT- $\mu$ (x5)	1,135k	92.43 ± 0.24	89.33 ± 0.31	91.55 ± 0.37	87.80 ± 0.39	92.63 ± 0.55	89.77 ± 0.35
AcT- $\mu$ (x10)	2,271k	<b>92.54 ± 0.21</b>	<b>89.79 ± 0.34</b>	<b>92.03 ± 0.33</b>	<b>88.02 ± 0.31</b>	<b>93.10 ± 0.53</b>	<b>90.22 ± 0.31</b>

TABLE IV

BENCHMARK OF DIFFERENT MODELS FOR SHORT-TIME HAR ON MPOSE2021 SPLITS USING POSENET 2D SKELETAL REPRESENTATIONS.

MPOSE2021 Split		PoseNet 1		PoseNet 2		PoseNet 3	
Model	Parameters	Accuracy [%]	Balanced [%]	Accuracy [%]	Balanced [%]	Accuracy [%]	Balanced [%]
Conv1D	4,062k	85.83 ± 0.71	79.96 ± 1.10	87.47 ± 0.35	78.51 ± 0.78	87.46 ± 0.67	81.31 ± 0.58
REMNet [1]	4,269k	84.75 ± 0.65	77.23 ± 0.94	86.17 ± 0.68	75.79 ± 1.30	86.31 ± 0.60	79.20 ± 0.79
ActionXPose [2]	509k	75.98 ± 0.72	64.47 ± 1.10	79.94 ± 1.10	67.05 ± 1.40	77.34 ± 1.40	66.86 ± 1.40
MLSTM-FCN [21]	368k	76.17 ± 0.84	64.75 ± 1.10	79.04 ± 0.72	65.62 ± 1.40	77.84 ± 1.30	67.05 ± 1.20
AcT- $\mu$	228k	86.66 ± 1.10	81.56 ± 1.60	87.21 ± 0.99	79.21 ± 1.60	87.75 ± 0.53	82.99 ± 0.87
AcT-S	1,042k	<b>87.63 ± 0.52</b>	<b>82.54 ± 0.87</b>	88.48 ± 0.57	81.53 ± 0.68	88.49 ± 0.65	83.63 ± 0.99
AcT-M	2,743k	87.23 ± 0.48	82.10 ± 0.66	<b>88.50 ± 0.51</b>	<b>81.79 ± 0.44</b>	<b>88.70 ± 0.57</b>	<b>83.92 ± 0.96</b>

(227k parameters) is able to extract general and robust features from temporal correlations in sequences. Increasing the number of parameters, a constant improvement in balanced accuracy can be observed for splits 3, while split 1 and 2 present oscillations. The difference between splits reflects how much information is conveyed by training sets and how much the model is able to learn from that. So, it is evident that AcT scales best on split three because there are complex correlations that a bigger model learns easier in that data. On the contrary, it seems AcT- $\mu$  is able to extract almost all the prone to generalize information from split 2, as the accuracy only slightly increases going towards more complex models.

As explained in II, ST-TR exploits an ensemble of two networks modeling spatial and temporal sequence correlations, respectively. Moreover, MS-G3D leverages further information such as skeleton graph connections and the position of bones. Ensembles are known to be very effective in reducing model variance, and they enhance performance by exploiting independent representations learned by each network, so it is unfair to compare them with single-shot architectures. For this reason, we create three ensemble versions of AcT- $\mu$  to have an even confront, with 2, 5, and 10 instances, respectively. The results reported at the bottom of III show that AcT- $\mu$  (x2) outperforms MS-G3D (J+B) in

all the benchmarks except for balanced accuracy in split 3, despite having less than one-tenth of its parameters. Finally, the ensembles of 5 and 10 AcT- $\mu$  instances achieve even higher accuracy on all the splits with only around 1 and 2 million parameters, respectively. That proves the balancing effect of ensemble enhances model predictions even without feeding the network with additional information.

As PoseNet data is mainly dedicated to real-time and Edge AI applications, only the models designed for this purpose have been considered in the benchmark, excluding MS-G3D, ST-TR, and AcT-L. In general, the results give similar insights. The tested models are the same as in the previous case, with all the necessary modifications given by the different input formats. In the MLP case, however, performance seriously degrades as networks strongly tend to overfit input data after a small number of epochs, so the results are not included in Table IV. That is caused by the fact that PoseNet is a lighter methodology developed for Edge AI and hence is more prone to noisy and even missing keypoint detections. That results in less informative data and emphasizes the difference between sequences belonging to different datasets, confusing the model and inducing it to learn very specific features as noise. The MLP is a too simple model that is particularly prone to this kind of problem.

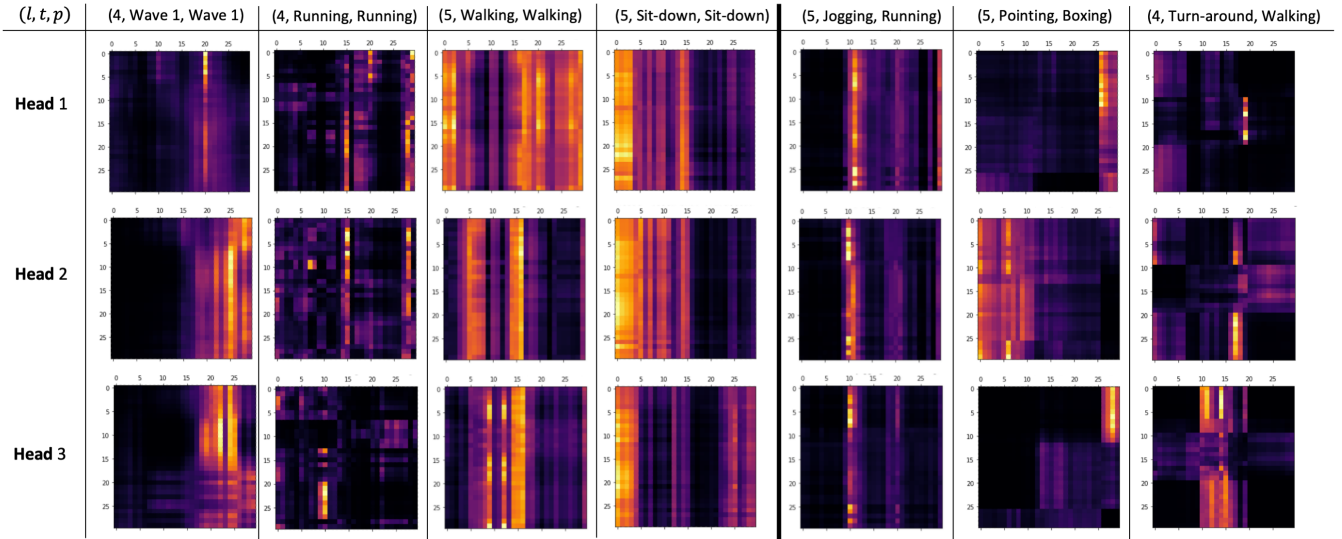


Fig. 6. Self-attention weights,  $A$ , of MPOSE2021 test samples.  $(l, t, p)$  represents the AcT-M  $l$ -th layer, the label and the prediction respectively. The three rightmost columns show three attention maps of a failed prediction and the other columns are from correct classifications. It is clear from all examples how the model focuses on certain particular frames of the series in order to extract a global representation of the scene.

Naturally, all the models are affected by the same problem, and the balanced accuracy on PoseNet is generally lower. The same considerations made for OpenPose apply in this case, where AcT outperforms all the other architectures and demonstrates its ability to give an accurate and robust representation of temporal correlations. Also, it is interesting to notice that Conv1D performs better than REMNet, proving to be less prone to overfitting, and that standard deviations are more significant than in the OpenPose case.

### C. Model Introspection

In order to have an insight into the frames of the sequence the AcT model attends to, we extract the self-attention weights at different stages of the network. In Fig. 6 MPOSE2021 test samples are propagated through the AcT-M model and attention weights,  $A$ , of the three distinct heads are presented. It can be seen that the model pays attention to specific frames of the sequence when a specific gesture defines the action. On the other hand, due to the distributed nature of actions such as walking and running, the attention of the model is much more spread across the different frames. Moreover, it is clear how the three heads mostly focus on diverse frames of the sequence. Finally, the rightmost columns show three attention maps of failed predictions. In these last cases, attention weights are less coherent with themselves, and the model is not capable of extracting a useful global representation of the scene.

Instead, in Fig. 7, the last layer self-attention score of the [CLS] token are shown together with the RGB and skeleton representations of the scene. Scores are the normalized sum of the three attention heads and give a direct insight into the frames exploited by AcT to produce the classification output. It can be seen that bent poses are much more informative for the model to predict the jumping in place action.

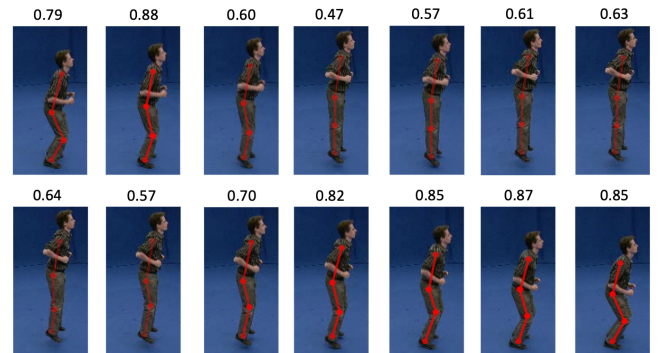


Fig. 7. Self-attention of the [CLS] token on the normalized heads sum of the last layer. Scores give a direct insight into the frames exploited by AcT to produce the classification output. The example clearly shows how bending positions are more insightful for the network to predict the jumping in place action. In the image, the attention score defines the skeleton alpha channel.

Moreover, we analyze the behavior of the network under a progressive reduction of the temporal information. That, as previously stated, can be easily done without retraining due to the intrinsic nature of the AcT model. In Fig. 8 is presented how the test-set balanced accuracy is affected by frame dropping. The two curves show a reduction starting from the beginning and end of the temporal sequence, respectively. It is interesting to notice how the performance of the AcT model degrades with an almost linear trend. That highlights the robustness of the proposed methodology and demonstrates the possibility of adapting the model to different applications requiring different temporal constraints.

Finally, we also study the positional embeddings of the AcT-M model by analyzing their cosine similarity, as shown in Fig. 9. Very nearby position embeddings demonstrate a high level of similarity, and distant ones are orthogonal or

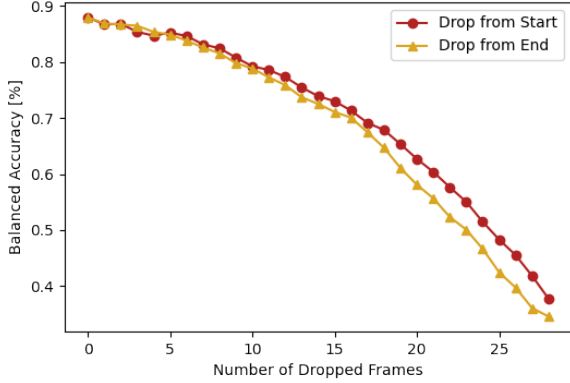


Fig. 8. AcT-M model test-set balanced accuracy with an incremental reduction of the temporal information. Due to the intrinsic nature of the network, it is possible to reduce the number of temporal step without a retraining or any kind of explicit adaptation.

in the opposite direction. This pattern is constant for all  $T$  frames of the sequence, highlighting how actions are not particularly localized and that relative positions are essential for all frames.

#### D. Latency Measurements

We also test the performance of all the considered models for real-time applications. To do so, we use the TFLite Benchmark<sup>3</sup> tool, which allows running TensorFlow Lite models on different computing systems and collecting statistical results on latency and memory usage. In our case, two CPUs are implied to measure model speed both on a PC and a mobile phone: an Intel i7-9700K for the former and the ARM-based HiSilicon Kirin 970 for the latter. In both experiments, the benchmark executes 10 warm-up runs followed by 100 consecutive forward passes, using 8 threads.

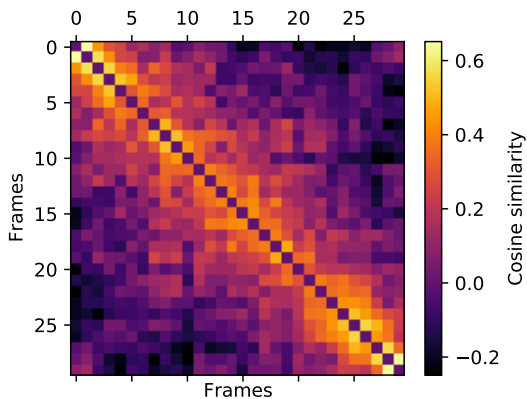


Fig. 9. Cosine similarities of the learned  $T$  position embeddings of AcT-M model.

<sup>3</sup><https://www.tensorflow.org/lite/performance/measurement>

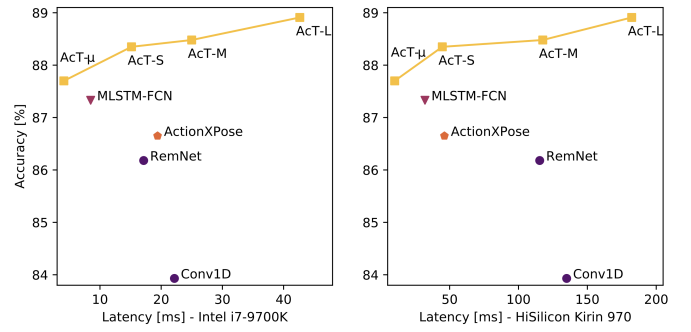


Fig. 10. Study of the latency of different tested models on a high-performance Intel CPU and on a mobile phone equipped with an ARM-based CPU.

The results of both tests are reported in Fig. 10, where only the MLP has been ignored because, despite being the fastest-running model, its accuracy results are much lower than its competitors. The graph shows the great computational efficiency of Transformer-based architectures, whereas convolutional and recurrent networks result in heavier CPU usage. Indeed, in the Intel i7 case, RemNet achieves almost the same speed as AcT-S, but its accuracy is 2% lower. Moreover, AcT- $\mu$  is able to outperform it, running at over four times its speed. MLSTM-FCN and ActionXPose, being smaller models, achieve lower latency than the baselines: the former stays between AcT- $\mu$  and AcT-S, while the latter performs similarly to AcT-S. These results are remarkable but still outperformed by AcT- $\mu$  both on accuracy and speed.

The difference with the baselines is even more evident on the ARM-based chip, as convolutional architectures seem to perform poorly on this kind of hardware. Indeed, RemNet and Conv1D run as fast as AcT-M with significantly lower accuracy, and AcT- $\mu$  is ten times quicker. Nothing changes for what concerns MLSTM-FCN and ActionXPose, with AcT- $\mu$  being more accurate and three times faster.

## VI. CONCLUSION

In this paper, we explored the direct application of a purely Transformer-based network to the action recognition problem. We introduced the AcT network, which significantly outperforms commonly adopted models for HAR with a simple and fully self-attentional architecture. In order to limit computational and energy requests, building on previous human action recognition and pose estimation research, the proposed methodology exploits 2D skeletal representations of short time sequences, providing an accurate and low latency solution for real-time applications. Moreover, we introduced MPOSE2021, a large-scale open-source dataset for short-time human action recognition, as an attempt to build a formal benchmark for future research on the topic. Extensive experimentation with our proposed methodology clearly demonstrates the effectiveness of the AcT model and poses the basis for meaningful impact on many practical computer vision applications. In particular, the great efficiency of AcT could be exploited for Edge AI, achieving good performance even on computationally limited devices.

Future work may further investigate the AcT architecture with 3D skeletons and long sequence inputs and attempt to include graph connections information in the input embeddings of the network.

## REFERENCES

- [1] S. Angarano, V. Mazzia, F. Salvetti, G. Fantin, and M. Chiaberge. Robust ultra-wideband range error mitigation with deep learning at the edge. *Engineering Applications of Artificial Intelligence*, 102:104278, 2021.
- [2] F. Angelini, Z. Fu, Y. Long, L. Shao, and S. M. Naqvi. Actionxpose: A novel 2d multi-view pose-based algorithm for real-time human action recognition. *arXiv preprint arXiv:1810.12126*, 2018.
- [3] F. Angelini, Z. Fu, Y. Long, L. Shao, and S. M. Naqvi. 2d pose-based real-time human action recognition with occlusion-handling. *IEEE Transactions on Multimedia*, 22(6):1433–1446, 2019.
- [4] F. Angelini and S. M. Naqvi. Joint rgb-pose based human action recognition for anomaly detection applications. In *2019 22th International Conference on Information Fusion (FUSION)*, pages 1–7. IEEE, 2019.
- [5] F. Angelini, J. Yan, and S. M. Naqvi. Privacy-preserving online human behaviour anomaly detection based on body movements and objects positions. In *ICASSP 2019-2019 IEEE International Conference on Acoustics, Speech and Signal Processing (ICASSP)*, pages 8444–8448. IEEE, 2019.
- [6] J. L. Ba, J. R. Kiros, and G. E. Hinton. Layer normalization. *arXiv preprint arXiv:1607.06450*, 2016.
- [7] I. Bello, B. Zoph, A. Vaswani, J. Shlens, and Q. V. Le. Attention augmented convolutional networks. In *Proceedings of the IEEE/CVF International Conference on Computer Vision*, pages 3286–3295, 2019.
- [8] A. Berg, M. O’Connor, and M. T. Cruz. Keyword transformer: A self-attention model for keyword spotting. *arXiv preprint arXiv:2104.00769*, 2021.
- [9] Z. Cao, G. Hidalgo, T. Simon, S.-E. Wei, and Y. Sheikh. Openpose: realtime multi-person 2d pose estimation using part affinity fields. *IEEE transactions on pattern analysis and machine intelligence*, 43(1):172–186, 2019.
- [10] M. Caron, H. Touvron, I. Misra, H. Jégou, J. Mairal, P. Bojanowski, and A. Joulin. Emerging properties in self-supervised vision transformers. *arXiv preprint arXiv:2104.14294*, 2021.
- [11] C. Chen, R. Jafari, and N. Kehtarnavaz. Utd-mhad: A multimodal dataset for human action recognition utilizing a depth camera and a wearable inertial sensor. In *2015 IEEE International conference on image processing (ICIP)*, pages 168–172. IEEE, 2015.
- [12] M. X. Chen, O. Firat, A. Bapna, M. Johnson, W. Macherey, G. Foster, L. Jones, N. Parmar, M. Schuster, Z. Chen, et al. The best of both worlds: Combining recent advances in neural machine translation. *arXiv preprint arXiv:1804.09849*, 2018.
- [13] S. Cho, M. Maqbool, F. Liu, and H. Foroosh. Self-attention network for skeleton-based human action recognition. In *Proceedings of the IEEE/CVF Winter Conference on Applications of Computer Vision*, pages 635–644, 2020.
- [14] J. Devlin, M.-W. Chang, K. Lee, and K. Toutanova. Bert: Pre-training of deep bidirectional transformers for language understanding. *arXiv preprint arXiv:1810.04805*, 2018.
- [15] A. Dosovitskiy, L. Beyer, A. Kolesnikov, D. Weissenborn, X. Zhai, T. Unterthiner, M. Dehghani, M. Minderer, G. Heigold, S. Gelly, et al. An image is worth 16x16 words: Transformers for image recognition at scale. *arXiv preprint arXiv:2010.11929*, 2020.
- [16] N. Gkalelis, H. Kim, A. Hilton, N. Nikolaidis, and I. Pitas. The i3dpost multi-view and 3d human action/interaction database. In *2009 Conference for Visual Media Production*, pages 159–168. IEEE, 2009.
- [17] L. Gorelick, M. Blank, E. Shechtman, M. Irani, and R. Basri. Actions as space-time shapes. *IEEE transactions on pattern analysis and machine intelligence*, 29(12):2247–2253, 2007.
- [18] D. Hendrycks and K. Gimpel. Gaussian error linear units (gelus). *arXiv preprint arXiv:1606.08415*, 2016.
- [19] S. Hochreiter and J. Schmidhuber. Long short-term memory. *Neural computation*, 9(8):1735–1780, 1997.
- [20] J. Hu, L. Shen, and G. Sun. Squeeze-and-excitation networks. In *Proceedings of the IEEE conference on computer vision and pattern recognition*, pages 7132–7141, 2018.
- [21] F. Karim, S. Majumdar, H. Darabi, and S. Harford. Multivariate lstm-fcns for time series classification. *CoRR*, 2018.
- [22] W. Kay, J. Carreira, K. Simonyan, B. Zhang, C. Hillier, S. Vijayanarasimhan, F. Viola, T. Green, T. Back, P. Natsev, et al. The kinetics human action video dataset. *arXiv preprint arXiv:1705.06950*, 2017.
- [23] B. Langmann, K. Hartmann, and O. Loffeld. Depth camera technology comparison and performance evaluation. In *ICPRAM (2)*, pages 438–444, 2012.
- [24] C.-H. Lin, E. Yumer, O. Wang, E. Shechtman, and S. Lucey. Stgan: Spatial transformer generative adversarial networks for image compositing. In *Proceedings of the IEEE Conference on Computer Vision and Pattern Recognition (CVPR)*, June 2018.
- [25] J. Liu, A. Shahroudy, M. Perez, G. Wang, L.-Y. Duan, and A. C. Kot. Ntu rgb+ d 120: A large-scale benchmark for 3d human activity understanding. *IEEE transactions on pattern analysis and machine intelligence*, 42(10):2684–2701, 2019.
- [26] Z. Liu, H. Zhang, Z. Chen, Z. Wang, and W. Ouyang. Disentangling and unifying graph convolutions for skeleton-based action recognition. In *Proceedings of the IEEE/CVF Conference on Computer Vision and Pattern Recognition*, pages 143–152, 2020.
- [27] I. Loshchilov and F. Hutter. Decoupled weight decay regularization. *arXiv preprint arXiv:1711.05101*, 2017.
- [28] G. Papandreou, T. Zhu, L.-C. Chen, S. Gidaris, J. Tompson, and K. Murphy. Personlab: Person pose estimation and instance segmentation with a bottom-up, part-based, geometric embedding model. In *Proceedings of the European Conference on Computer Vision (ECCV)*, pages 269–286, 2018.
- [29] C. Plizzari, M. Cannici, and M. Matteucci. Skeleton-based action recognition via spatial and temporal transformer networks. *Computer Vision and Image Understanding*, 208:103219, 2021.
- [30] C. Schuldt, I. Laptev, and B. Caputo. Recognizing human actions: a local svm approach. In *Proceedings of the 17th International Conference on Pattern Recognition, 2004. ICPR 2004.*, volume 3, pages 32–36. IEEE, 2004.
- [31] A. Shahroudy, J. Liu, T.-T. Ng, and G. Wang. Ntu rgb+ d: A large scale dataset for 3d human activity analysis. In *Proceedings of the IEEE conference on computer vision and pattern recognition*, pages 1010–1019, 2016.
- [32] L. Shi, Y. Zhang, J. Cheng, and H. Lu. Skeleton-based action recognition with directed graph neural networks. In *Proceedings of the IEEE/CVF Conference on Computer Vision and Pattern Recognition*, pages 7912–7921, 2019.
- [33] L. Shi, Y. Zhang, J. Cheng, and H. Lu. Two-stream adaptive graph convolutional networks for skeleton-based action recognition. In *Proceedings of the IEEE/CVF Conference on Computer Vision and Pattern Recognition*, pages 12026–12035, 2019.
- [34] L. Song, G. Yu, J. Yuan, and Z. Liu. Human pose estimation and its application to action recognition: A survey. *Journal of Visual Communication and Image Representation*, page 103055, 2021.
- [35] N. Srivastava, G. Hinton, A. Krizhevsky, I. Sutskever, and R. Salakhutdinov. Dropout: a simple way to prevent neural networks from overfitting. *The journal of machine learning research*, 15(1):1929–1958, 2014.
- [36] H. Touvron, M. Cord, M. Douze, F. Massa, A. Sablayrolles, and H. Jégou. Training data-efficient image transformers & distillation through attention. *arXiv preprint arXiv:2012.12877*, 2020.
- [37] A. Vaswani, N. Shazeer, N. Parmar, J. Uszkoreit, L. Jones, A. N. Gomez, L. Kaiser, and I. Polosukhin. Attention is all you need. *arXiv preprint arXiv:1706.03762*, 2017.
- [38] D. Weinland, R. Ronfard, and E. Boyer. Free viewpoint action recognition using motion history volumes. *Computer vision and image understanding*, 104(2-3):249–257, 2006.
- [39] L. Xia, C.-C. Chen, and J. K. Aggarwal. View invariant human action recognition using histograms of 3d joints. In *2012 IEEE computer society conference on computer vision and pattern recognition workshops*, pages 20–27. IEEE, 2012.
- [40] S. Yan, Y. Xiong, and D. Lin. Spatial temporal graph convolutional networks for skeleton-based action recognition. In *Proceedings of the AAAI conference on artificial intelligence*, volume 32, 2018.